Melanoaging: Uncovering and resolving an age-spot specific metabolic change and cellular senescence caused by excessive melanin deposition

Daigo Inoue[1], Alif Meem Nurani[1], Katsuyuki Maeno[1], Kumiko Kikuchi[1], Aoki Hirofumi[1], Tomoko Onodera[1], Takako Shibata[1]

[1]MIRAI Technology Institute, Shiseido Co., Ltd., Yokohama, Japan

ABSTRACT

Introduction

Solar lentigo (hereafter called age spot) is one of the major symptoms of photoaging in which extrinsic and intrinsic factors such as UV irradiation, melanogenesis, and abnormal keratinocyte-turnover are involved. Difficulties to obtain live skin-tissues of age-spot lesions have limited its investigation to the identification of implicating factors instead of clarifying the overall environment that causes age-spot formation and maintenance. Here we aimed to develop a novel non-invasive measurement approach to verify the age spot environment at a cellular level *in vivo* and uncover a key integrative pathway for age-spot specific senescence process, "melanoaging". By uncovering melanoaging, we further identified active ingredients that radically improve age spots.

Methods

For identifying key factors in age spots, epidermis of both age spots and non-lesion areas were subjected to proteomics analysis. Effect of excessive melanin

1

deposition on the metabolic shift of mitochondria in cultured keratinocytes was analyzed by real-time metabolic flux analyzer and immunohistochemical analysis. To confirm the role of cellular metabolic shift *in vivo*, non-invasive measurement of NAD(P)H fluorescent lifetime decay in the granular layer of either age-spot or non-lesion area were carried out by fluorescence lifetime imaging microscopy, FLIM. We further investigated whether excessive melanin-deposition directly causes inflammation and senescence in melanin-stored keratinocytes by immunohistochemical and biochemical analyses. Melanin-stored keratinocytes treated with active ingredients were analyzed by metabolic shift assays, as well as inflammation and senescence markers to confirm their effect on melanoaging pathway.

Results

Non-invasive measurement of fluorescence lifetime decay of NAD(P)H in live age-spots demonstrated that oxidative-phosphorylation (OXPHOS) of mitochondria in the epidermal granular layer was significantly downregulated compared to that in non-lesion areas. Further, the expression of mitochondrial proteins related to OXPHOS were significantly downregulated in the epidermis of age spots. At a cellular level, excessive melanin-deposition arrested the cell cycle of basal keratinocytes in a dose dependent manner, dramatically downregulating OXPHOS in differentiating keratinocytes. Moreover, excessive melanin deposition induced early senescence by cell-cycle arrest, and the onset of late senescence by secreting inflammatory factors. Our results provide novel evidence that excessive-melanin deposition causes cellular metabolic changes and facilitates age-spot specific senescence process referred to as

2

"melanoaging". As a radical solution targeting melanoaging, certain active ingredients were significantly able to improve OXPHOS downregulation and senescence phenotypes induced by excessive melanin, suggesting that such combination of active ingredients may possibly restore proper KC differentiation and turnover regardless of excessive melanin deposition. Based on these findings, we suggest a pragmatic age-spot care targeting melanoaging that prevents the aggravation of age spots by improving its deteriorated microenvironment.

Discussion and Conclusion

The difficulty of obtaining fresh age-spot specimens have limited age-spot research to UV-irradiated phenotypes of epidermal cells, and thus their solutions mostly targeted prevention of melanogenesis and melanin deposition. Additionally, conventional non-invasive measurements for age spots, have mainly focused on the melanin content as an index. Our FLIM measurement procedure, for the first time, revealed a pivotal process forming age spot environment that involves metabolic shift and senescence induced by excessive melanin deposition. Hence, we suggest that melanoaging is crucial for the age-spot life stage: formation, maintenance, and expansion of age spots. Finally, we successfully developed new efficacies of active ingredients that target the comprehensive process of melanoaging: OXPHOS metabolic dysfunction and senescence leading to age spot-specific abnormal differentiation of melanin-accumulated KCs. Our research on melanoaging will be a paradigm shift for developing pragmatic solutions targeting respective life stages of age spots.

INTRODUCTION

Age spots is one of the earliest signs of photoaging where chronic UV exposure on sun-exposed areas of skin such as faces and back of the hands forms asymmetric hyperpigmented lesions. Typically, small age spots appear on the cheek at the age of 30s, which gradually expand or get darker around 40s-50s [1]. Even though, extensive research has been conducted in academia and industry for decades to cure age spots, it still stands as a major skin concern for consumers, affecting their perceived age as the most conspicuous aging phenotype. Nonetheless, radical cure of age spots remains almost unattainable, due to reappearance even after aesthetic medical treatments as well as disparity in efficacy of anti-pigmentary cosmetic solutions towards each age spot. One plausible reason is the lack of understanding of the life cycle of age spot, despite enormous knowledge on what factors contribute to the emergence of age spots. The mechanisms of the onset of hyperpigmentation converge on two major abnormalities: upregulation of melanogenesis and melanocyte dendricity and excessive deposition of basal keratinocytes (KCs) [2][3]. Interestingly, the number of melanocytes does not significantly appear to increase in both non-lesion and age spots, suggesting that there may exist mechanisms in KCs for establishment and maintenance of the hyperpigmented

4

state [2][3]. In fact, enhanced expression of various inflammatory and hormonal factors such as GM-CSF, α-MSH, Endothelin-1, occurs in KCs which further stimulate melanin by facilitating the expression of melanogenesis-related factors, tyrosinase, TRP1, and MITF [4] [5]. In turn, basal KCs chronically store excessive melanin by forming perinuclear melanin-cap [6]. The aforementioned abnormalities being attributed to chronic UV exposure, it is still unclear what differentiates the emergence of age spots from non-lesional neighboring area even with similar history of UV exposure. Additionally, while excessive melanin-deposition in age spots could function as protective parasol of KCs from UV-induced DNA damage, a longstanding discrepancy remains on why KCs with excessive melanin maintain adverse inflammatory/melanocytic environment. A clue to address those problems resides in a modulated fate of melanin-deposited basal KCs where abnormal differentiation underlies initiation of age-spot formation. Previous studies indicate that the downregulation of either E-cadherin or Notch1 results in abnormal differentiation, activating downstream inflammatory/melanocytic factors thereby specifying age-spot environment [7][8]. Hence, besides UV exposure as an extrinsic factor, it requires consideration of previously undescribed intrinsic factors, which could establish and maintain age spots. An unaddressed issue is how turnover of excessive melanin-deposited KCs to stratum corneum can be achieved despite abnormal differentiation in age spots. Similar to non-lesion area, there is an abrupt reduction of deposited melanin in KCs during transition from basal to differentiating layer in age spots [9][10]. The enigma of this process implies that the environment of entire epidermis in age spots is constitutively maintained

even after exit of melanin-deposited KCs by epidermal turnover. Therefore, revealing intrinsic abnormality of excessive melanin-deposited KCs would resolve not only emergence of age spots, but also how the hyperpigmented state is established and maintained, providing a comprehensive understanding of the age spot life cycle.

Limited availability of skin samples containing age spots from either aesthetic plastic surgery or postmortem specimens hinders to tackle the above-mentioned problems. To overcome this issue, non-invasive measurement in age spots has been long sought [11][12][13]. For example, optical coherence tomography (OCT) angiography revealed abnormal microvascular structure in dermis of age spots, which could play a pivotal role in forming inflammatory milieu [11]. Additionally, fluorescence lifetime imaging microscopy (FLIM), which measures the lifetime decay of autofluorescence of endogenous molecules such as melanin, NAD(P)H, and certain vitamins, visualized the extent of melanin content and distribution in skin [14]. In light of such prior attempts, we speculated that fluorescence lifetime imaging could allow us to define an age-spot specific molecular fingerprint and demonstrate efficacies of active ingredients that pragmatically improve milieu of age spots. However, non-invasive measurement of endogenous fluorophores such as NAD(P)H and FAD in age spots has been challenging due excessive melanin deposition in basal KCs [15].

The assessment of cellular metabolic state by FLIM can be applied to investigate the degree of pleiotropic aging processes in skin [16][17]. For

6

instance, distinctive fluorescence lifetime decays of protein-free and -bound NAD(P)H provide indirect information on two metabolic states, mitochondria oxidative phosphorylation (OXPHOS) and cytoplasmic glycolysis, respectively [18]. OXPHOS is crucial for the large sum of ATP consumption during KC differentiation in contrast with basal KCs where glycolysis prevails [19][20], raising a possibility that metabolic dysfunction may occur either systemically or locally in age spots. Since metabolic dysfunction mediated by OXPHOS downregulation tightly links to senescence process [21], it is plausible that age spots may also display an age-spot specific senescence-like pattern with pleiotropic inflammatory/melanocytic factors. Anti-aging research including photoaging, sagging and wrinkles has multifacetedly investigated the senescence of both KCs and fibroblasts [22][23], however such approach for improving age spots has not been sufficiently explored, possibly due to limited advancement of senescence knowledge in age spots [24].

Here we aimed to develop a novel non-invasive measurement approach to verify the age spot microenvironment at a cellular level and uncover a key integrative pathway for age-spot specific intrinsic process, "melanoaging". In melanoaging, excessive melanin deposition in KCs induced downregulation of OXPHOS and partially arrested proliferation of KCs, followed by the secretion of cellular senescence factors. By uncovering melanoaging, we further identified active ingredients specifically targeting melanin-deposited KCs. Additionally, the efficacy of the combination of three active ingredients was evaluated by FLIM, demonstrating that the ingredient complex significantly improved age spots by

7

not only improving OXPHOS metabolism of differentiated KCs but also the senescence state of excessive melanin-deposited KCs.

Materials and Methods

Non-invasive measurement procedure of cellular metabolism in age spots by multiphoton laser tomography and FLIM analysis

The study was approved by the Shiseido Ethics Committee (approval number: C10290, C10382 and B10430). A written informed consent was obtained from all participants. 18 participants (12 female, 6 male) aged 30-69 with distinguished hyperpigmented lesions on cheeks, all identified as solar lentigo by a dermatologist were recruited. For assessment of clinical efficacy of a complex ingredient, 19 female participants aged 40-59 with age spots on both sides of cheeks were carefully recruited. Participants applied two types of serums Placebo and a triple active ingredient 4MSK/TA/GK2 (1% 4MSK (potassium methoxysalicylate), 2%TA (tranexamic acid), 0.05% GK2 (dipotassium glucyrrhizate)) separately on each side of the face for 6 weeks. Measurement was performed on one spot area and one peripheral non-lesion area to compare their metabolic activity. *In vivo* skin measurement was conducted by clinical multiphoton tomographies using MPTcompact (JenLab) at a fixed wavelength of 780 nm and MPTflex (JenLab) at 760 nm excitation wavelength and a maximum power of 10 mW. Fluorescence lifetime analysis was performed using Symphotime 64 (PicoQuant) and SPCImage software (Becker&Hickl) for the cytoplasm of cells in the granular layer of epidermis. The

8

fluorescence decay curves were fitted using either bi- or tri-exponential decay model depending on the experimental data. We analyzed 3-5 regions of interest (ROI) in the cell cytoplasm for each FLIM image. Phasor plots were analyzed to distinguish any mixed species contaminating the NAD(P)H lifetime components. Amplitude of bound NADPH lifetime to free NADPH lifetime ($A_{bound\ NADPH}$/$A_{free\ NADPH}$) values were calculated to determine the metabolic shift.

Preparation of melanin-deposited cultured KCs

Synthetic melanin (M0418, Sigma-Aldrich) was dissolved in 1x PBS at the final concentration of 1% (w/v) and sonicated at room temperature for 2h. Sonicated melanin was diluted to various final concentrations (0.001-0.01%) with Epilife cultured medium (MEPI500CA, Thermo Fisher Scientific). Cultured KCs were incubated with melanin-dissolved medium for 12h. The cultures were washed twice with 1xPBS to remove residual melanin not phagocytosed into KCs. Melanin-deposited KCs were further investigated for downstream analyses.

Screening of chemical ingredients for improving both mitochondria metabolism and senescence in melanin-deposited KCs

About 50 chemical compounds were primarily selected based on their individual efficacies to promote epidermal turnover, KC differentiation or barrier function along with correspondence to mitochondrial metabolism. Melanin-deposited KCs (0.004% melanin) at a cell density of 5×10^5 cells/well were prepared in a 24-well plate. Individual ingredients diluted in cultured medium at various final concentration were added to the cells and incubated for 2 more days, followed

by induction of differentiation by adding 1.8 mM $CaCl_2$. After 1d of differentiation, total ATP production by OXPHOS of either control or ingredient-treated KCs was analyzed by Glycolysis/OXPHOS assay kit (G270, DOJINDO) as manufacture's instruction. The screened ingredients from this assay were further evaluated for secondary screening as follows. Basal melanin-deposited KCs treated with screened ingredients were incubated for 5 days without replacing the medium. The supernatants of the culture were analyzed with Lumit®HMGB1 human/mouse immunoassay (W6110, Promega) and Human CXCL1/GRO alpha Quantikine ELISA Kit (DGR00B, RD Systems). The total ATP production was normalized relative to the total viable cell number of the individual samples.

Assessment of solar lentigines and human cutaneous specimens

Commercial facial cutaneous specimens (Obio LLC. and CTIBiotech) containing hyperpigmented lesions were used to assess the histological features of age spots, such as rete ridge, hyperpigmentation in basal KCs, and thickened epidermis. The selected samples (n=5, two males and three females, 79–91 years of age) were embedded in paraffin to prepare histological sections and subjected to immunofluorescence, to examine the expression patterns of Ki67, GROα, COX7C, cytochrome c and other proteins.

Cell cultures

Normal human epidermal KCs (Kurabo) from Caucasian, Asian, African neonatal foreskin were cultured in EpiLife medium supplemented with HuMedia KG Growth Factor Kit (KK-6150, Kurabo). For viable cell counting, the

fluorescence of either the alamarBlue cell viability reagent (DAL1025, Thermo

Fisher Scientific) or Hoechst 33258 was measured using the multi-detection

microplate reader (POWERSCAN HT, BioTek).

Measurement of oxidative consumption rate (OCR) by Flux Analyzer

OCR of either melanin-deposited basal KCs or melanin-deposited differentiating

KCs in individual optimized media was measured by Flux Analyzer (Agilent

Technologies) as manufacture's instruction.

Gene expression analysis

Total RNAs of either melanin-deposited or control KCs were purified using

RNeasy spin columns (74104, Qiagen) as manufacture's instruction. The

labeled cRNA probes were applied to a human on-slide synthesized oligo DNA

microarray (Whole Human Genome Oligo Array G4112A, Agilent

Technologies). Scanning and data acquisition were performed as described

previously [25].

Sample preparation and liquid chromatography-tandem mass
spectrometry (LC-MS/MS)

EasyPep™ 96 MS Sample Prep Kit (Thermo Fisher Scientific) was used for

sample preparation for LC-MS/MS, including lysate preparation as

manufacture's instruction. An Ultimate 3000 RSLCnano system (Thermo Fisher

Scientific) and Orbitrap Fusion Lumos (Thermo Fisher Scientific) were utilized

for LC-MS/MS analysis. The analysis employed a nano-HPLC capillary column

(ODS, 75 µm i.d. x 120 mm, particle size: 3.0 µm, Nikkyo Technos Co Ltd,

Tokyo, Japan). A linear gradient of 2−35 % mobile phase B (0.1% formic acid in

acetonitrile) over 120 min was utilized for peptide separation, with mobile phase A consisting of 0.1% formic acid in water. A data-dependent acquisition mode was employed to trigger precursor isolation and sequencing. All raw LC-MS/MS analysis used Proteome Discoverer (version 2.3). Sequest and Amanda databases were utilized with MS/MS spectra searched against the Swiss-Prot and TrEMBL human databases. Label-free quantitation (LFQ) calculations were performed separately for each parameter group containing similar cell loadings, utilizing unique and razor peptides. Gene ontology (GO) enrichment analysis was performed using Metascape [26].

Statistical analysis

Data are presented as mean±standard deviation. Statistical analyses were performed by Prism 7 (GraphPad), using Student's t-test (paired, two-tailed) or multiple comparisons (one-way, two-way ANOVA) based on the experimental data. Differences with a value of $p < 0.05$ were considered statistically significant.

Immunofluorescence of cutaneous tissues and cultured cells

Fixed cultured cells and paraffin sections of cutaneous tissues were prepared as previously described [27]. Static images of the immunostained samples were retrieved with a 20× objective, using confocal microscopy (LSM700 and LSM880, ZEISS) and further analyzed using ImageJ. The imaging data for the statistical analyses were binarized and measured using ImageJ.

Primary antibodies against the following were used: COX7C (11411-2-AP, Proteintech), cytochrome c (ab11032, abcam), Ki67(ab92742, abcam), COXIV (ab109863, abcam), GROα (12335-1-AP, Proteintech), and HMGB1 (ab18256,

abcam), CINtec p16 Histology (705-47, Roche), and p21 Waf1/Cip1 (2947T, Cell Signaling technology). The secondary antibodies used were Alexa Fluor™ 488-conjugated anti-mouse or anti-rabbit IgG (A11001, A21206, Thermo Fisher Scientific) and Alexa Fluor™ 647-conjugated anti-mouse or anti-rabbit IgG (A21236, A21245, Thermo Fisher Scientific).

RESULTS

Metabolic downregulation of epidermis in age spots

To investigate the microenvironment of epidermis in live skin, we performed fluorescent lifetime tomography between age spots and neighboring non-lesion areas. Since the fluorescent-lifetime decay of free NAD(P)H in the basal and suprabasal (spinous layer) layers is difficult to segregate from that of deposited melanin in KCs, we first assessed the granular layer immediately under the stratum corneum (Fig.1A), which has been reported to have less contribution of melanin [13]. The fluorescence lifetime of NAD(P)H in its free form is usually observed around 0.2-1.2 ns, while bound form of NAD(P)H has a longer lifetime range from 1ns-6.5 ns [28]. The lifetime itself fluctuates, depending on the cellular environment such as pH, binding proteins, binding conformations or even the total NAD(P)H pool [29][30]. Recent reports have revealed that the ratio of amplitude of long lifetime to short lifetime of NAD(P)H ($A_{bound\ NADPH}/A_{free\ NADPH}$) is a precise indicator of the redox state of cells [30], hence, we used this parameter to determine there is any change in cellular metabolism in age spots and neighboring non-lesions. Indeed, the $A_{bound\ NADPH}/A_{free\ NADPH}$ value was

13

significantly downregulated in age spots, suggesting that oxidative phosphorylation (OXPHOS) was reduced compared to that of non-lesions (Fig.1B). Our results indicate for the first time that, such a downregulation of OXPHOS occurring in the differentiated layer may contribute to the dysfunctional differentiation status of age spots.

To investigate a mechanistic clue for OXPHOS downregulation in age spots, we next addressed the protein compositions in age spot epidermis, confirmed by the expression of age-spot specific markers, relative to neighboring non-lesion areas by proteomic analysis. About 4400 proteins that were differentially expressed in age spots were further narrowed down to identify any proteins related with mitochondrial metabolism. GO enrichment analysis revealed that aerobic respiration including OXPHOS, electron transport chain, and tricarboxylic acid cycle was statistically clustered in age spots (Fig.1C). Differential expression patterns of mitochondria-related proteins further identified mitochondrial proteins COX7C and cytochrome c, associated with ATP production by electron transport chain, were significantly suppressed by 1.5-2-fold in age spots (Fig.1C). In fact, immunofluorescence of COX7C and cytochrome c exhibited weaker expression pattern of both proteins in age spot epidermis, corroborating the results of proteomics analysis (Fig.1D). Together with the results from FLIM analysis, these results indicated that mitochondrial metabolism in epidermis is constitutively downregulated at a protein level in age spots.

Suppression of KC proliferation via melanin deposition

14

Mitochondrial metabolism is tightly linked to KC cell fate, balancing between cellular proliferation and differentiation [31]. To understand the connection between age spot specific metabolic dysfunction and abnormal differentiation, we asked whether excessive melanin-deposition affects mitochondrial metabolism, thereby modulating KC proliferation/differentiation. To address this, we first investigated the proliferative state of melanin-deposited KCs in the basal layer. The ratio of Ki67-positive basal cells with melanin-cap was significantly lower than that of Ki67-positive basal cells without melanin-cap in age spots, suggesting that melanin-deposited KCs are less proliferative (Fig.2A). These results raised a possibility that melanin-deposition prevents proliferation of KCs. To test this, we next utilized a melanin-deposition model (Fig.2B, top panels), in which basal KCs phagocytose synthetic melanin, to form perinuclear melanin-cap [32]. The size of the melanin-cap proportionally and significantly increased with over 0.004-0.005% melanin (hereafter utilized to assess for excessive melanin-deposition) in a concentration dependent manner (Fig. 2B). The proliferative activity of melanin-deposited keratinocytes was also inhibited at higher melanin concentrations (Fig.2C). In support of these results, DNA microarray analysis with this model confirmed that various cell-cycle activators such as cyclin B, D, and E were suppressed, and expressions of cell-cycle inhibitors p21 and p15 were promoted in melanin-deposited KCs (Fig.2D). Our results collectively indicated that melanin-deposition leads to suppression of KC proliferation by targeting cell-cycle activators/inhibitors.

Downregulation of mitochondrial metabolism via melanin deposition during KC differentiation

In the previous section, we clarified that excessive melanin deposition suppressed KC proliferation. We next examined for any metabolic dysfunction in KCs caused by excessive melanin deposition. Since transition from basal to differentiating KCs accompanies distinct metabolic shift from glycolysis to OXPHOS (Fig.3A), both basal and differentiating KCs were examined for oxidative consumption rate (OCR) in the presence and absence of melanin. In basal KCs, the activity of mitochondrial respiration measured by OCR as well as total ATP production was comparable between untreated and melanin-deposited KCs (Fig.3B). In contrast, after induction of KC differentiation, both ATP production and OCR were significantly repressed in the presence of melanin (Fig.3C). In fact, consistent with proteomics analysis and immunostaining of age-spot epidermis (Fig.1C, D), reduced expression levels for both COX7C and cytochrome c were observed in melanin-deposited KCs after 2 days of differentiation. Meanwhile, expression of an ubiquitous mitochondrial protein, COXIV, was comparable to that of control, suggesting that melanin deposition specifically perturbed OXPHOS metabolism. Taken together, these results suggested that melanin-deposition prevents OXPHOS metabolism possibly by downregulating mitochondrial proteins involved in the electron transport chain.

Melanoaging: Senescence-like pattern of excessive melanin-deposited KCs

Acute inhibition of both OXPHOS and cellular proliferation by excessive melanin-deposition in cultured KCs were consistent with the results of *in vivo* imaging and whole tissue analysis of age spots (Fig.1, 2 and 3). We next asked whether such mitochondrial dysfunction and proliferation arrest due to excessive melanin deposition can subsequently induce a senescence-like phenotype in KCs. As a rather late event, KCs analyzed after 5 days of melanin deposition showed significant increase in nuclear localizations of both p21 and nuclear p16 than control basal KCs (Fig.4A, B). As cell-cycle arrest is linked to early senescence [33], these results suggested that melanin deposition induces early senescence in a p21/p16-dependent manner. We further examined late senescence process, involving the secretion of senescence-associated secreted phenotype (SASP) [33]. Elevated levels of two SASP proteins [34], HMGB1 and GROα were observed in the supernatants from melanin-deposited KCs relative to control (Fig.4C), indicating that certain SASP factors are implicated in the late senescence-like phenotype. *In vivo*, it is difficult to observe stable senescence patterns of KCs due to active epidermal turnover of basal keratinocytes and exit from the stratum corneum [35]. We speculated that excessive melanin-deposition may slow down turnover and thus may accumulate SASPs in KCs. Indeed, expression of GROα protein was upregulated in the epidermis of age spots (Fig.4D), suggesting that melanin-deposition leads to accumulated secretion pattern. Conclusively, we provide mechanistic evidence that melanin dependent OXPHOS downregulation, and senescence-like pattern of epidermis is a characteristic feature in age spots, hereafter called "melanoaging" as an age-spot specific aging process.

17

Identification of active ingredient complex (4MSK/TA/GK2) targeting melanoaging

Melanoaging involves two age-spot specific cellular processes, OXPHOS downregulation and cellular senescence, and targeting melanoaging would be a strategic approach to effectively improve the age-spot microenvironment. To achieve this, we set out to screen ingredients that can improve both OXPHOS downregulation and senescence microenvironment in melanin-deposited KCs (Fig.5A). Melanin treatment alone showed downregulation of OXPHOS-mediated ATP production in contrast with untreated control KCs. Among 30 potential active ingredients, dipotassium glucyrrhizate (hereafter called GK2) and glucosyl hesperidin, were significantly able to upregulate OXPHOS-mediated ATP production (Fig.5B). These two candidates were further screened for a potential inhibitory effect on secreted senescence marker HMGB1(Fig. 5C) Interestingly, GK2, but not glucosyl hesperidin, remarkably suppressed the secretion of HMGB1 from melanin-deposited KCs. In fact, GK2 is known to possess inhibitory activity against HMGB1 [36]. Further, we found that combination of GK2 with two other active ingredients, tranexamic acid (TA) and potassium methoxysalicylate (4MSK) (hereafter as 4MSK/TA/GK2) inhibited GROα secretion in a cumulative manner (Fig. 5D). These sequential screening strongly demonstrated that 4MSK/TA/GK2 is an effective ingredient complex that targets melanoaging.

Effect of 4MSK/TA/GK2 for improving age spots *in vivo*

To assess if 4MSK/TA/GK2 can improve the age spot microenvironment, we conducted a continuous use test without (Placebo) or with 4MSK/TA/GK2-formulated serum on each side of the face for 6 weeks and measured the metabolic activity of age spots and neighboring non-lesions on both sides by FLIM (Fig. 6A). At week 0, $A_{bound\ NADPH}/A_{free\ NADPH}$ was downregulated in age spots relative to neighboring non-lesion areas, consistent with our previous result (Fig.6B and also see Fig. 1B). Interestingly, use of 4MSK/TA/GK2 formulation, but not Placebo, significantly upregulated $A_{bound\ NADPH}/A_{free\ NADPH}$ at week 6, suggesting amplified OXPHOS activity in both age spots and non-lesions (Fig. 6C). Our results provide novel evidence that 4MSK/TA/GK2 formulation efficiently increases OXPHOS metabolism in live age spots.

Based on our findings from *in vitro* and *in vivo* efficacy studies, we suggest that 4MSK/TA/GK2 targets the melanoaging process by improving both the senescence state of melanin-deposited KCs as well as the attenuated metabolic activity of age spots' microenvironment.

DISCUSSION

Beyond individual age-spot factors: Uncovering radical microenvironment of age spots at cellular level by non-invasive measurement

The difficulty of obtaining fresh age-spot samples has restricted the analysis of real time changes in living tissues. Non-invasive measurement techniques, such as reflectance confocal microscopy (RCM) and OCT angiography have

successfully visualized microstructures in age spots [11][37], but it remains challenging to deep dive into the dynamic changes of molecular events at cellular level. One example is the FLIM measurement procedure, where high concentration of melanin in the basal and suprabasal layers, hinders quantification of metabolic activity in skin [15]. However, by focusing on the state of NAD(P)H in the granular layer, we successfully identified a change in cellular metabolism, OXPHOS downregulation in age spots.

Given that current trends in age spot research focus on individual factors and their complicity in major signaling pathways such as melanogenesis, inflammation, and turnover, regardless, they simply overview age spots from a particular lens and timepoint, failing to provide a comprehensive picture of the age-spot life cycle [25][38][39]. Thus, current solutions do not fulfill the demand of customers possessing diverse shapes, sizes and the life stage of age spots (Fig.7). Our integrative approach using non-invasive measurement techniques combined with whole-tissue proteomics, for the first time, revealed real time changes of cellular processes in age spots, thereby providing mechanistic insights into an age-spot specific aging process in the life stage of age spots (Fig.7). This leaves us a groundbreaking clue about how age spots are established and maintained, by conserving the age-spot specific microenvironment, which will be discussed in the next section.

Melanoaging; Intrinsic aging pattern in age spots

Our results of a systemic downregulation of OXPHOS in epidermis of age spots

provided intriguing distinction since OXPHOS is generally upregulated in KCs

upon UV irradiation by promoting KC proliferation/differentiation [40]. One

possible explanation could be drawn from our *in vivo* and *in vitro* analyses that

melanin deposition downregulates OXPHOS during differentiation but not in

basal stem cell state (Fig.3B, C). Cutaneous diseases such as actinic keratosis

and seborrheic keratosis that exhibit proliferation/differentiation defects of

keratinocytes in epidermis are implicated to be maintained by keratinocyte

senescence [41][42]. However, the involvement of senescent KCs remains

obscure in age spots. Senescent cultured basal KCs induced by UVB

irradiations may promote melanin-uptake, but it does not suffice to answer

whether melanin accumulated keratinocytes are senescent. Our present study

introduces an intrinsic senescent process of age spots, melanoaging, caused by

excessive melanin-deposition in KCs. While melanin functions as a scavenger

of radical species and shields KCs against UV-mediated DNA damage, physical

and long-term effects of perinuclear melanin on KCs have not been well

addressed so far. In fact, suppression of KC proliferation due to melanin or

melanosome deposition is suggested as a function for making time to repair

DNA damage [43]. On the contrary, particle matter 2.5 (PM2.5) elicits cell-cycle

arrest and senescence in KCs, reminiscent of the similar resultant effect of

phagocytosed melanin presented here [44]. Additionally, in Parkinson disease,

neuromelanin forms macular aggregates complexed with heavy ions and

proteins, exacerbating the deteriorated environment for the disease [45]. Since

physiological condition of KCs in the skin basal layer do not have chance to

ingest such artificial molecules and neuromelanin, we speculate that excessive melanin deposition could be recognized as a physical alerting signal that hinders homeostasis of KCs. From a different perspective, concentration dependent negative impact of melanin-deposition raises a concern whether darker skin types may also have an analogous effect. We confirmed that the consequence of excessive melanin-deposition is irrespective of skin types (data not shown), implying that even though there exists a different threshold among diverse ethnic groups, excessive melanin deposition may be posing a long-term adverse effect. In support of this, recent studies indicate that melanin acts as a photosensitizer by UV irradiation and chemical stimuli in a long-term aspect, affecting the homeostasis of KCs and melanocytes, leading to apoptosis and melanoma [46][47]. In future, it requires consideration on how different types of melanin such as eumelanin and pheomelanin, intrinsically have a long-term impact on skin homeostasis in diverse ethnic groups.

Anti-melanoaging solutions for pragmatic care of age spots

Current understanding of age spots has advanced development of solutions targeting both epidermis and dermis layers. In the dermis, targeting fibroblast senescence, microvascular formation, nerve fibers, and melanophage have been suggested despite the challenge to pragmatically approach the dermis by topical application of cosmetic solutions. In epidermis, most cosmetic ingredients block melanogenesis or facilitate epidermal turnover [48]. However, it appears not to suffice the radical improvement due to only targeting a part of the systemic environment of age spots. Melanoaging process in epidermis

22

underlies such melanocytic environment, which have not yet been approached by current ingredients. Based on melanoaging theory, we specifically screened ingredients against melanin-deposited KCs, successfully identifying that GK2, an ingredient for anti-roughness of skin, promotes metabolic activity of KCs. Furthermore, combined with two anti-hyperpigmentary ingredients 4MSK and TA [49], 4MSK/TA/GK2 can cumulatively suppress melanoaging. In this synergistic effect, GK2 could serve as a powerhouse supplying energy to cells while 4MSK/TA plays an active role by reducing SASP factors and melanin, thereby improving the overall age-spot microenvironment (Fig. 5 and 6). From our clinical efficacy studies, we speculate that 4MSK/TA/GK2 may also protect neighboring non-lesions from deteriorating into an age spot-like milieu in the future. Such a combinational approach to target both melanoaging and hyperpigmentation for the first time by 4MSK/TA/GK2 provided a concrete ground on how strategic selection of ingredient complexes and correct formulations can surpass their individual potential as age-spot solutions. Lastly, utilizing non-invasive and non-labeled measurement methods not only for mechanistic research but for clinical efficacy of our ingredients, we hereby set an example for next generation age-spot research that for the first time addresses the complex life cycle of age spots. We believe that targeting melanoaging may help prevent aggravation of age spots eventually improving the deteriorated state of both the epidermal and dermal environment, reversing the aging process (Fig.7). Finally, we conclude that the concept of melanoaging goes beyond age-spot research and can be applied to elucidate various aging

processes in individuals, and develop pragmatic solutions that contemplate heterogeneity and diversity of consumers.

CONCLUSIONS

Using non-invasive multiphoton tomography to investigate facial age spots, for the first time, we uncovered a pivotal axis forming age spot environment, melanoaging, that involves metabolic dysfunction and senescence patterns induced by excessive melanin deposition. Melanoaging could help resolve unanswered questions about the life cycle of age spots: how age spots appear, expand or get darker. While current age-spot solutions mostly target melanogenesis pathways, we successfully developed formulations that improve melanoaging, which may allow us to pragmatically control hyperpigmentation by targeting the age spot specific milieu. Our research on melanoaging will be a paradigm shift that changes the future of aging research and help us explore the possibility of unprecedented solutions ensuring radical age spot care.

Conflict of Interest Statement

The authors declare no conflicts of interest.

REFERENCES

1. Kikuchi K, Masuda Y, Yamashita T, et al., A new quantitative evaluation method for age-related changes of individual pigmented spots in facial skin. *Skin Res Technol*. Aug;22(3):318-324 (2016).

2. Cario-Andre M, Lepreux S, Pain C, et al., Perilesional vs. lesional skin changes in senile lentigo. *J Cutan Pathol*. Jul;31(6):441-447 (2004).

3. Unver N, Freyschmidt-Paul P, Hörster S, et al., Alterations in the epidermal-dermal melanin axis and factor XIIIa melanophages in senile lentigo and ageing skin. *Br J Dermatol*. Jul;155(1):119-128 (2006).

4. Otręba M, Rok J, Buszman E, et al., Regulation of melanogenesis: the role of cAMP and MITF. *Postepy Hig Med Dosw*. 66:33-40 (2012).

5. D'Mello SA, Finlay GJ, Baguley BC, et al., Signaling Pathways in Melanogenesis. *Int J Mol Sci*. 17:1144 (2016).

6. Nguyen NT, Fisher DE. MITF and UV responses in skin: From pigmentation to addiction. *Pigment Cell Melanoma Res*. 32:224-236 (2019).

7. Inoue D, Narita T, Ono T, et al., A mechanism of melanogenesis mediated by E-cadherin downregulation and its involvement in solar lentigines. *Int J Cosmet Sci*. Dec;45(6):775-790 (2023).

8. Barysch MJ, Braun RP, Kolm I, et al., Keratinocytic Malfunction as a Trigger

for the Development of Solar Lentigines. *Dermatopathology*. 6:1-11 (2019).

9. Noblesse E, Nizard C, André MC, et al., Skin ultrastructure in senile lentigo. *Skin Pharmacol Physiol*. 19(2):95-100 (2006).

10. Lin CB, Hu Y, Rossetti D, Chen N, et al., Immuno-histochemical evaluation of solar lentigines: The association of KGF/KGFR and other factors with lesion development. *J Dermatol Sci.* Aug;59(2):91-97 (2010).

11. Hara Y, Yamashita T, Ninomiya M, et al., Vascular morphology in facial solar lentigo assessed by optical coherence tomography angiography. *J Dermatol Sci*. Jun;102(3):193-195 (2021).

12. Yamashita T, Negishi K, Hariya T, et al., In vivo microscopic approaches for facial melanocytic lesions after quality-switched ruby laser therapy: time-sequential imaging of melanin and melanocytes of solar lentigo in Asian skin. *Dermatol Surg*. Jul;36(7):1138-1147 (2010).

13. Pena AM, Decencière E, Brizion S, et al., In vivo melanin 3D quantification and z-epidermal distribution by multiphoton FLIM, phasor and Pseudo-FLIM analyses. *Sci Rep*. Jan 31;12(1):1642 (2022).

14. Datta R, Heaster TM, Sharick JT, et al., Fluorescence lifetime imaging microscopy: fundamentals and advances in instrumentation, analysis, and applications. *J Biomed Opt*. May;25(7):1-43 (2020).

15. Ung TPL, Lim S, Solinas X, et al., Simultaneous NAD(P)H and FAD fluorescence lifetime microscopy of long UVA-induced metabolic stress in reconstructed human skin. *Sci Rep*. Nov 12;11(1):22171 (2021).

16. Sanchez WY, Obispo C, Ryan E, et al., Changes in the redox state and

endogenous fluorescence of in vivo human skin due to intrinsic and photo-aging, measured by multiphoton tomography with fluorescence lifetime imaging. *J Biomed Opt*. Jun;18(6):061217 (2013).

17. Koehler MJ, Preller A, Elsner P, et al., Non-invasive evaluation of dermal elastosis by in vivo multiphoton tomography with autofluorescence lifetime measurements. *Exp Dermatol*. Jan;21(1):48-51 (2012).

18. Ouyang Y, Liu Y, Wang ZM, et al., FLIM as a Promising Tool for Cancer Diagnosis and Treatment Monitoring. *Nanomicro Lett*. Jun 3;13(1):133 (2021).

19. Stringari C, Abdeladim L, Malkinson G, et al., Multicolor two-photon imaging of endogenous fluorophores in living tissues by wavelength mixing. *Sci Rep*. Jun 19;7(1):3792 (2017).

20. Pouli D, Balu M, Alonzo CA, et al., Imaging mitochondrial dynamics in human skin reveals depth-dependent hypoxia and malignant potential for diagnosis. *Sci Transl Med*. Nov 30;8(367):367ra169 (2016).

21. Kwon SM, Hong SM, Lee YK, et al., Metabolic features and regulation in cell senescence. *BMB Rep.* Jan;52(1):5-12 (2019).

22. Zhang J, Yu H, Man MQ, et al., Aging in the dermis: Fibroblast senescence and its significance. *Aging Cell*. Feb;23(2):e14054 (2024).

23. Chin T, Lee XE, Ng PY, et al., The role of cellular senescence in skin aging and age-related skin pathologies. *Front Physiol*. Nov 22;14:1297637 (2023).

24. Goorochurn R, Viennet C, Granger C, et al., Biological processes in solar lentigo: insights brought by experimental models. *Exp Dermatol*. Mar;25(3):174-177 (2016).

25. Aoki H, Moro O, Tagami H, et al., Gene expression profiling analysis of solar

lentigo in relation to immunohistochemical characteristics. *Br J Dermatol*. Jun;156(6):1214-1223 (2007).

26. Zhou Y, Zhou B, Pache L, et al., Metascape provides a biologist-oriented resource for the analysis of systems-level datasets. *Nat Commun*. Apr 3;10(1):1523 (2019).

27. Inoue D, Narita T, Ono T, et al., A mechanism of melanogenesis mediated by E-cadherin downregulation and its involvement in solar lentigines. *Int J Cosmet Sci*. Dec;45(6):775-790 (2023).

28. Malak M, James J, Grantham J, et al., Contribution of autofluorescence from intracellular proteins in multiphoton fluorescence lifetime imaging. *Sci Rep*. Oct 5;12(1):16584 (2022).

29. Leben R, Köhler M, Radbruch H, et al., Systematic Enzyme Mapping of Cellular Metabolism by Phasor-Analyzed Label-Free NAD(P)H Fluorescence Lifetime Imaging. *Int J Mol Sci*. Nov 7;20(22):5565 (2019).

30. Song A, Zhao N, Hilpert DC, et al., Visualizing subcellular changes in the NAD(H) pool size versus redox state using fluorescence lifetime imaging microscopy of NADH. *Commun Biol*. Apr 9;7(1):428 (2024).

31. Hamanaka RB, Chandel NS. Mitochondrial metabolism as a regulator of keratinocyte differentiation. Cell Logist. Jan 1;3(1):e25456 (2013).

32. Pajak S, Hopwood LE, Hyde JS, et al., Melanin endocytosis by cultured mammalian cells. A model for melanin in a cellular environment. *Exp Cell Res*. Dec;149(2):513-526 (1983).

33. Liao Z, Yeo HL, Wong SW, et al., Cellular Senescence: Mechanisms and Therapeutic Potential. *Biomedicines*. Nov 25;9(12):1769 (2021).

34. Basisty N, Kale A, Jeon OH, Kuehnemann C, et al., A proteomic atlas of senescence-associated secretomes for aging biomarker development. *PLoS Biol*. Jan 16;18(1):e3000599 (2020).

35. Ho CY and Dreesen O. Faces of cellular senescence in skin aging. *Mech Ageing Dev*. 198:111525 (2021).

36. Vitali R, Palone F, Cucchiara S, et al., Dipotassium Glycyrrhizate Inhibits HMGB1-Dependent Inflammation and Ameliorates Colitis in Mice. *PLoS One*. Jun 19;8(6):e66527 (2013).

37. Farabi B, Khan S, Jamgochian M, et al., The role of reflectance confocal microscopy in the diagnosis and management of pigmentary disorders: A review. *J Cosmet Dermatol*. Dec;22(12):3213-3222 (2023).

38. Yamada T, Hasegawa S, Inoue Y, et al., Comprehensive analysis of melanogenesis and proliferation potential of melanocyte lineage in solar lentigines. *J Dermatol Sci* Mar;73(3):251-257 (2014).

39. Odawara M, Mezaki M, Yoshimura T, et al., Epidermal turnover and iron metabolism in senile lentigo. *J Dermatol*. Mar;51(3):453-457 (2024).

40. Hegedűs C, Boros G, Fidrus E, et al., PARP1 Inhibition Augments UVB-Mediated Mitochondrial Changes-Implications for UV-Induced DNA Repair and Photocarcinogenesis. *Cancers (Basel)*. Dec 18;12(1):5 (2019).

41. Chin T, Lee XE, Ng PY, et al., The role of cellular senescence in skin aging and age-related skin pathologies. *Front Physiol*. Nov 22;14:1297637 (2023).

42. Bajaji A, Senescence, Keratinisation, Latency: Seborrheic Keratosis. *Ann*

Med & Surg Case Rep: AMSCR: 100002 (2019)

43. Calapre L, Gray ES, Kurdykowski S, et al., Heat-mediated reduction of apoptosis in UVB-damaged keratinocytes in vitro and in human skin ex vivo. *BMC Dermatol*. May 26;16(1):6 (2016).

44. Herath HMUL, Piao MJ, Kang KA, et al., Hesperidin Exhibits Protective Effects against PM2.5-Mediated Mitochondrial Damage, Cell Cycle Arrest, and Cellular Senescence in Human HaCaT Keratinocytes. *Molecules*. Jul 27;27(15):4800 (2022).

45. Vila M. Neuromelanin, aging, and neuronal vulnerability in Parkinson's disease. *Mov Disord*. Oct;34(10):1440-1451 (2019).

46. Yamaguchi Y, Takahashi K, Zmudzka BZ, et al., Human skin responses to UV radiation: pigment in the upper epidermis protects against DNA damage in the lower epidermis and facilitates apoptosis. *FASEB J*. Jul;20(9):1486-1488 (2006).

47. Díaz DFZ, Busch L, Kröger M, et al., Significance of melanin distribution in the epidermis for the protective effect against UV light. *Sci Rep*. Feb 12;14(1):3488 (2024).

48. Maeda K. Timeline of the Development of Skin-Lightening Active Ingredients in Japan. *Molecules*. Jul 26;27(15):4774 (2022).

49. Ando H, Matsui MS, Ichihashi M, Quasi-drugs developed in Japan for the prevention or treatment of hyperpigmentary disorders. *Int J Mol Sci.* Jun 18;11(6):2566-2575 (2010).
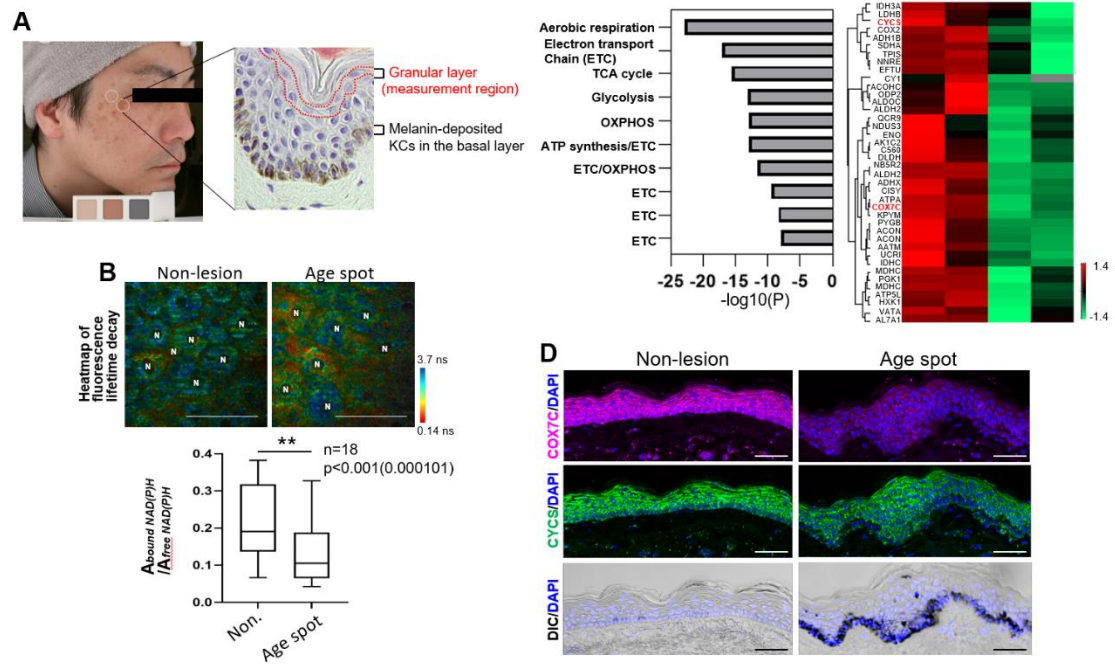
Figure 1

Figure 1 | Metabolic downregulation of epidermis in age spots. **A**, A schematic diagram of the measurement area of facial age spot and neighboring non-lesion (left panel, dashed circle). Cells at the granular layer (dashed red line) was measured by FLIM (see Materials and Methods). **B**, Representative heat map of fluorescence lifetime decay in individual cells of either non-lesion or age spot (top panels, N; Nucleus). The ratio of amplitude of protein-bound NAD(P)H to free NAD(P)H ($A_{bound\ NA(P)DH}/A_{free\ NAD(P)H}$) was significantly decreased in age spots. **C**, GO enrichment analysis showing statistical cluster of proteins related to aerobic respiration in age spots (left panel). A heatmap view of the expression pattern of mitochondria-related proteins in the epidermis of either non-lesions or age spots by mass spectrometry (n=2 each). COX7C and CYCS examined in Fig.1D are labeled in red. **D**, Representative decreased expressions of COX7C and Cytochrome c (CYCS) in age spots compared to neighboring non-lesional areas (n=5). DIC; Images of $\underline{D}$ifferential $\underline{I}$nterference $\underline{C}$ontrast. Scale bars, 50 µm (**B**, **D**). The data represents median with Min-Max.
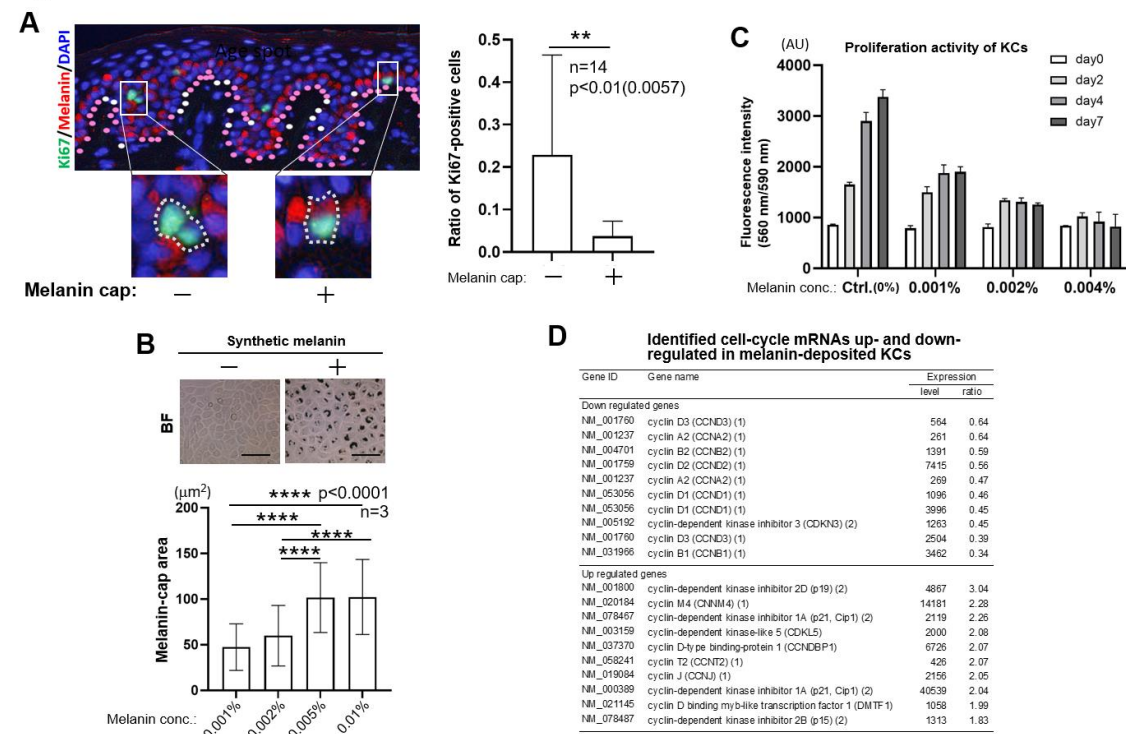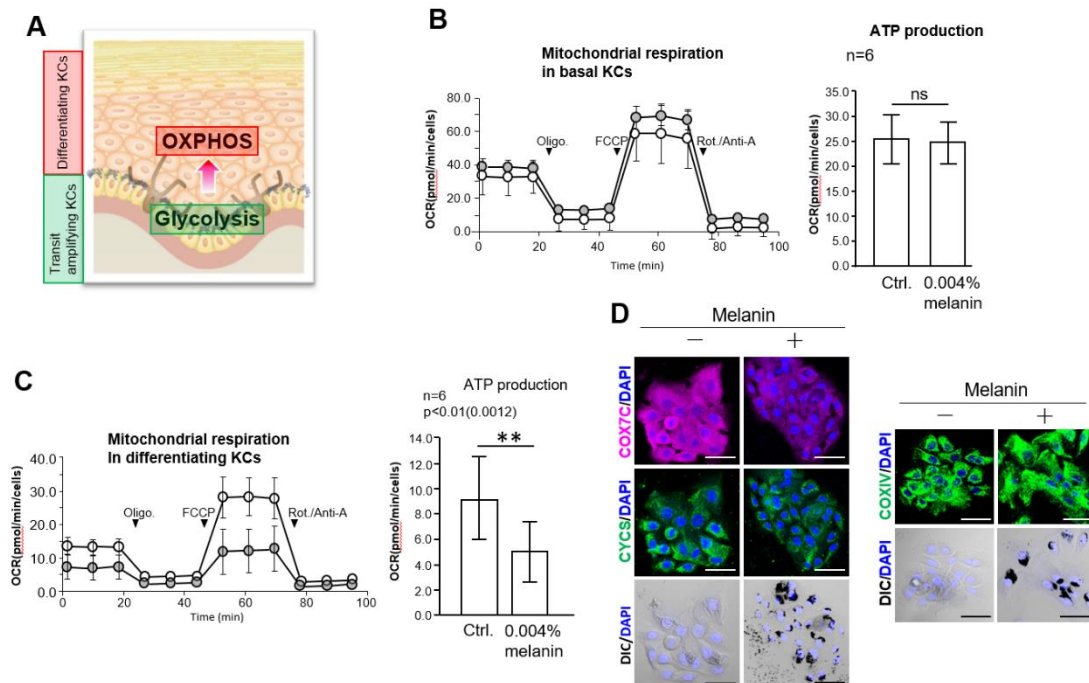
Figure 2

Figure 2 | Suppression of keratinocyte proliferation due to excessive melanin-deposition. A, Schematic classification of Ki67-positive KCs with (pink dots) or without melanin cap (white dots, left inset) in age spots (left panel, right inset). Ratio of Ki67-positive KCs was significantly decreased in melanin-deposited KCs in age spots. **B**, KCs with or without synthetic melanin-cap as a melanin-deposited KC model (Top panels). The area of perinuclear melanin cap was significantly increased at higher doses of melanin **C**, Decreased proliferation of melanin-deposited KCs in a melanin-concentration dependent manner. **D**, Down- and up-regulated cell-cycle proteins in melanin-deposited KCs by DNA-microarray analysis. BF; Bright field. Scale bars, 50 μm. The data represents mean±SD.

32

Figure 3 | Downregulation of mitochondrial metabolism in melanin-
Figure 3

deposited differentiating KCs. A, Schematic representation of metabolic state of KCs in epidermis. **B**, **C**, Mitochondrial respiration measured by oxygen consumption rate (OCR) with serial applications of mitochondrial respiration modulators (Oligomycin (Oligo.), FCCP, and Rotenone/Antimycin A (Rot./Anti-A)) (left), and ATP production derived from mitochondria (OXPHOS) (right) in either basal (**B**) or differentiating (**C**) KCs. ATP production was significantly decreased in differentiating melanin-deposited KCs but not in basal melanin-deposited KCs. **D**, Representative decreased expression of OXPHOS-related mitochondrial proteins COX7C and CYCS melanin-deposited KCs compared to control KCs. The expression of ubiquitous mitochondrial protein COXIV, was comparable to that of control. DIC; Images of Differential Interference Contrast. Scale bars, 50 μm (**D**). The data represents mean±SD.
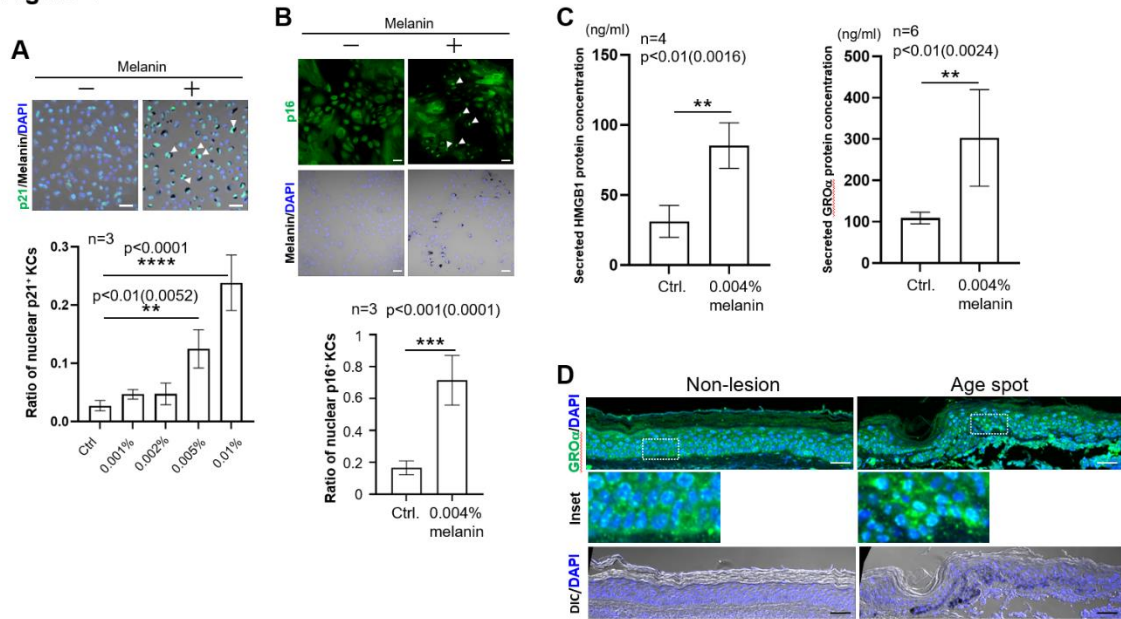
Figure 4

Figure 4 | Senescence-like pattern due to excessive melanin-deposition: Melanoaging. A, Melanin-dose dependent increase of nuclear p21-positive KCs (top panels, white arrowheads). **B**, Increase of nuclear p16-positive KCs in excessive melanin (0.004%)-deposited KCs (top panels, white arrowheads). **C**, Secretion of SASP proteins, HMGB1 and GROα increased in the supernatant of excessive melanin-deposited KCs. **D**, Representative increased GROα expression in age spots compared to neighboring non-lesion areas (n=5). Scale bars, 50 μm (**A, B, D**). The data represents mean±SD.
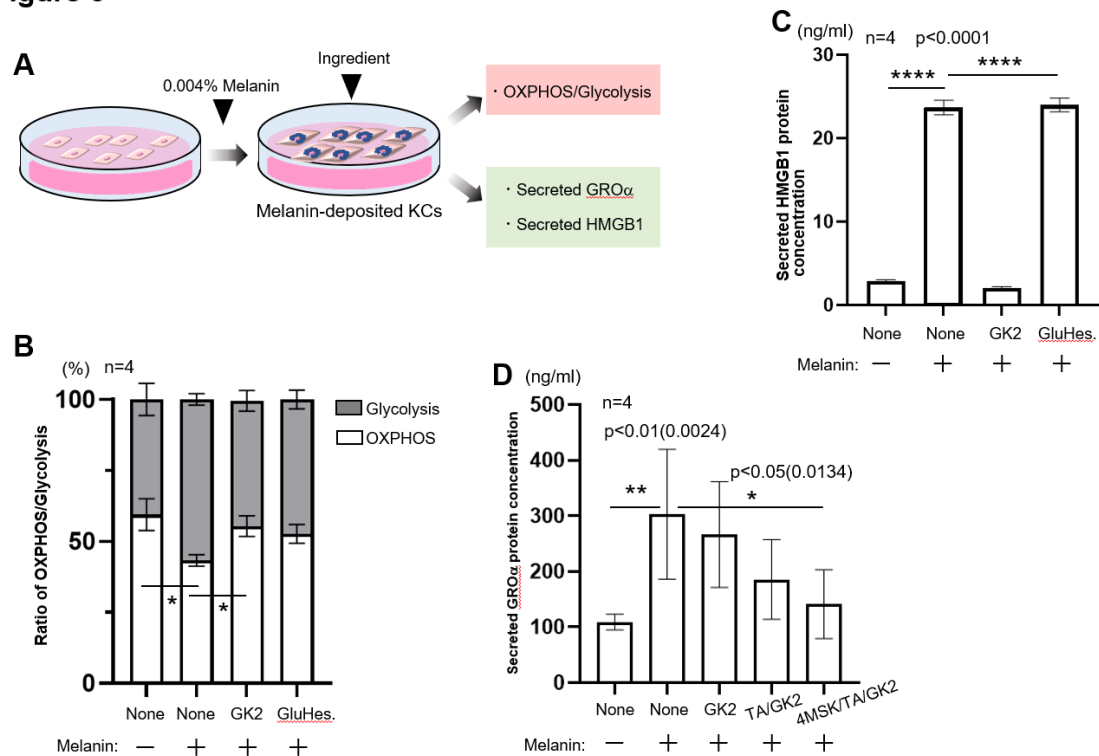
Figure 5

Figure 5 |Identification of active ingredient complex (4MSK/TA/GK2) targeting melanoaging. A, A schematic illustration of ingredient screening in melanin-deposited KCs. After the addition of individual ingredient, OPXHOS/Glycolysis ratio, and secretions of HMGB1 and GROα proteins were investigated (see details in Materials and Methods). **B**, Enhanced ratio of OXPHOS activity in GK2 and glucosyl hesperidin (GluHes.)-treated KCs even in the presence of excessive melanin. **C**, GK2, but not GluHes., inhibited the secretion of HMGB1 from melanin-deposited KCs. **D**, Cumulative add-on effect of 4MSK/TA/GK2 in blocking GROα secretion from melanin-deposited KCs. The data represents mean±SD.
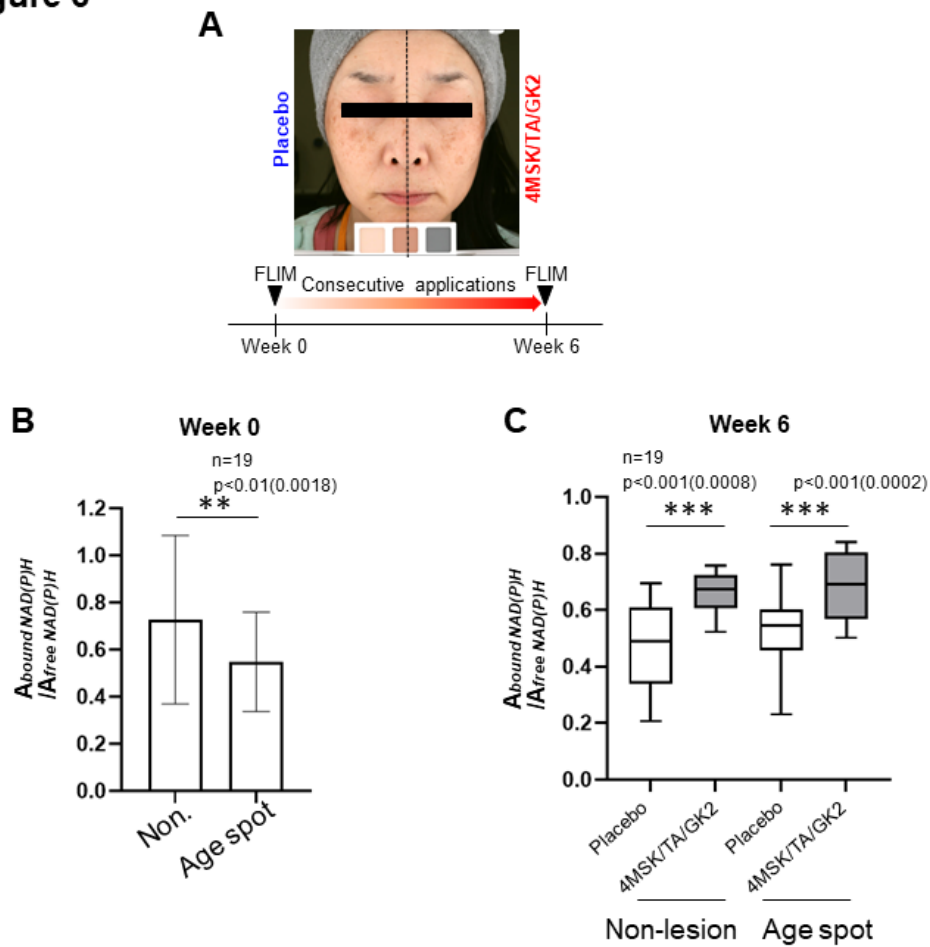
Figure 6

Figure 6 | Effect of triple ingredient complex 4MSK/TA/GK2 for improving age spots. A, A schematic of measurement procedure for examining clinical efficacy of 4MSK/TA/GK2 (see Materials and Methods). **B**, $A_{bound\ NAD(P)H}/A_{free\ NAD(P)H}$ was reduced in age spots compared to neighboring non-lesions at week 0. **C**, At week 6 after the consecutive applications, $A_{bound\ NAD(P)H}/A_{free\ NAD(P)H}$ was significantly increased in both non-lesions and age spots treated with 4MSK/TA/GK2 but not Placebo. The data represents mean±SD (**B**) and median with Min-Max (**C**).
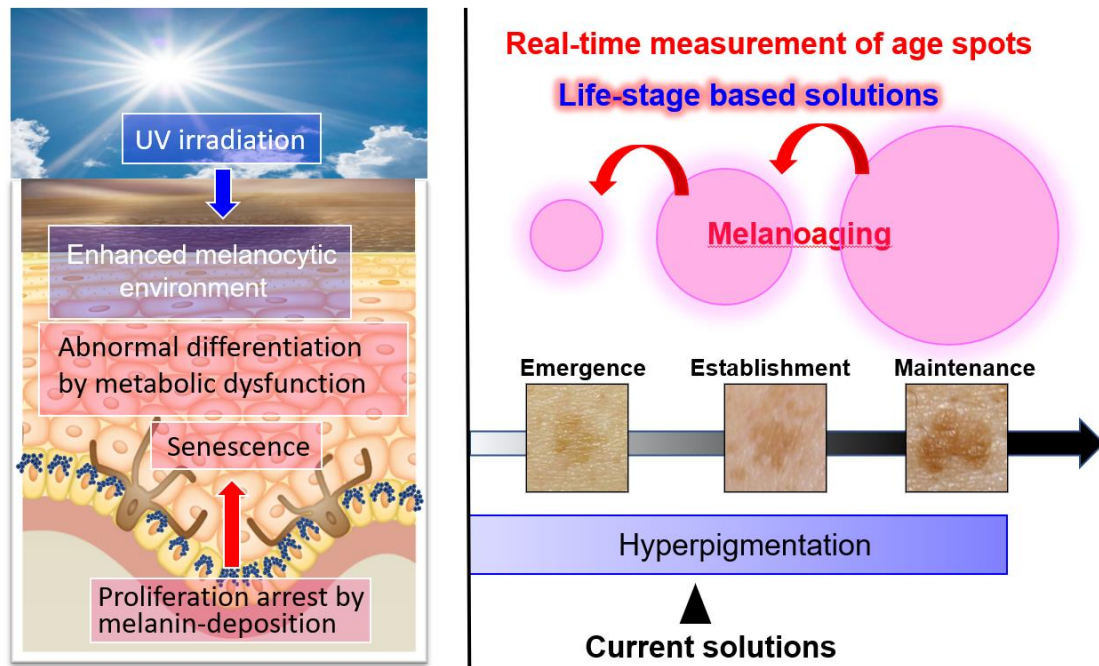
Figure 7

Figure 7 | A schematic of melanoaging in the life stage of age spots and perspective of solutions. Age spots occur from extrinsic triggers like chronic UV irradiation, developing an enhanced melanocytic environment. After melanin-deposition, there is an intrinsic risk of melanoaging, which causes cell-cycle arrest, abnormal differentiation by metabolic dysfunction, and senescence. Melanoaging explains how age-spot milieu is established and maintained. By real time imaging and measurement, we can decode the life cycle of age spots and develop customized solutions for each life stage. In near future, we hope to reverse the aggravation process and propose radical cure of age spots.